

**JOUL, Volume 2**

**Supplemental Information**

**Phase Boundary Mapping to Obtain *n*-type**

**Mg<sub>3</sub>Sb<sub>2</sub>-Based Thermoelectrics**

**Saneyuki Ohno, Kazuki Imasato, Shashwat Anand, Hiromasa Tamaki, Stephen Dongmin Kang, Prashun Gorai, Hiroki K. Sato, Eric S. Toberer, Tsutomu Kanno, and G. Jeffrey Snyder**

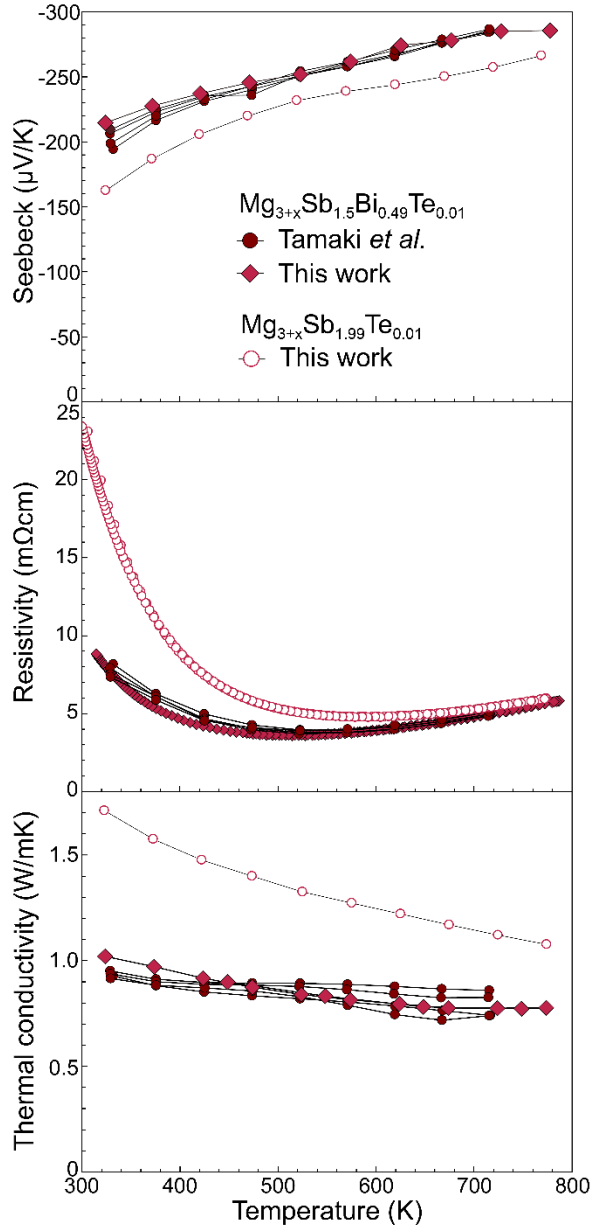


Figure S1. Transport properties of  $\text{Mg}_{3+x}\text{Sb}_{1.5}\text{Bi}_{0.49}\text{Te}_{0.01}$  and  $\text{Mg}_{3+x}\text{Sb}_{1.99}\text{Te}_{0.01}$  synthesized in this work with the data of  $\text{Mg}_{3+x}\text{Sb}_{1.5}\text{Bi}_{0.49}\text{Te}_{0.01}$  reported in ref [6]. Thermal conductivity of  $\text{Mg}_{3+x}\text{Sb}_{1.5}\text{Bi}_{0.49}\text{Te}_{0.01}$  and  $\text{Mg}_{3+x}\text{Sb}_{1.99}\text{Te}_{0.01}$  are calculated with the experimentally determined heat capacity reported in ref [6 and 31]. Reproduced  $\text{Mg}_{3+x}\text{Sb}_{1.5}\text{Bi}_{0.49}\text{Te}_{0.01}$  shows almost identical properties to the reported  $\text{Mg}_{3+x}\text{Sb}_{1.5}\text{Bi}_{0.49}\text{Te}_{0.01}$ .

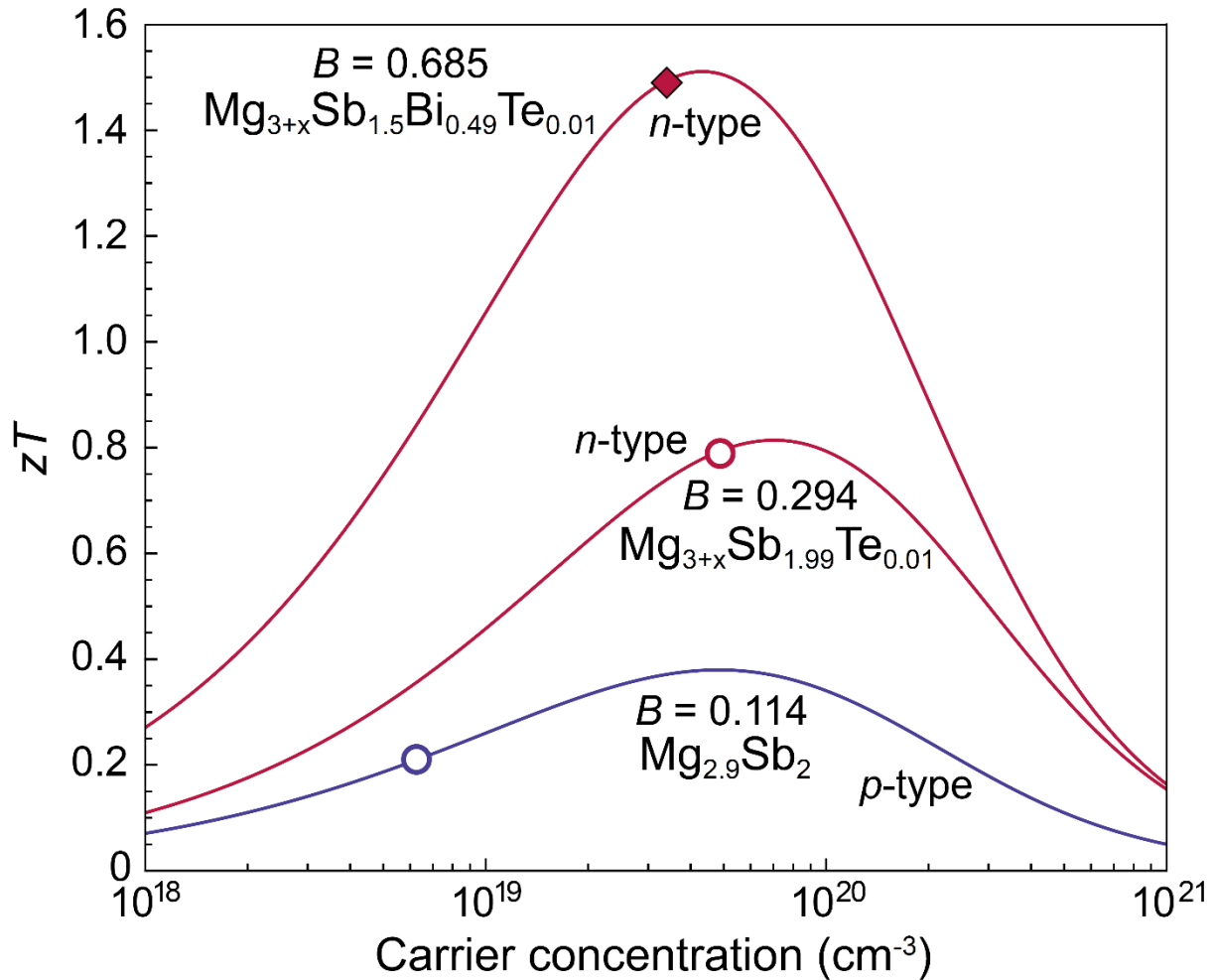


Figure S2. The predicted  $zT$  of  $\text{Mg}_3\text{Sb}_2$ -based materials as a function of Hall carrier concentration. Solid curves are obtained from experimental data (symbols) based on an effective  $m^*$  model. At 715 K, it is safe to assume the acoustic phonon scattering. The  $n$ -type  $\text{Mg}_3\text{Sb}_2$  is predicted to be superior thermoelectric material to  $p$ -type due to the multiband effect. 0.2 at. % of Te doping realizes the almost optimum doping level for all of the  $n$ -type samples.  $B$  is a dimensionless material quality factor, which shows the potential of the material as thermoelectric.  $\text{Mg}_3\text{Sb}_2$  can possess about 2.5 times higher  $B$  just by being  $n$ -type conduction and it becomes even higher by alloying.

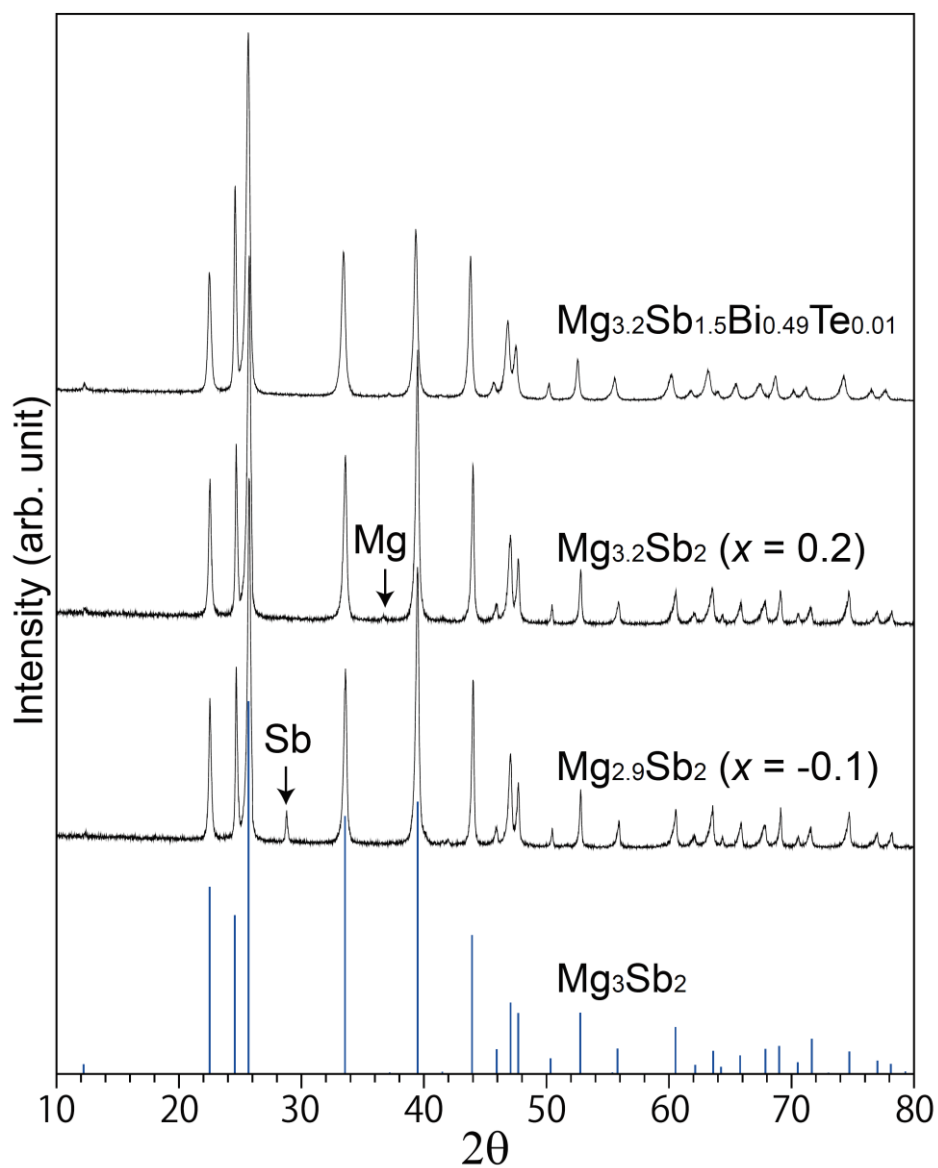


Figure S3. Lab XRD patterns of the hot-pressed  $\text{Mg}_3\text{Sb}_2$ -based compounds with theoretical pattern of  $\text{Mg}_3\text{Sb}_2$  (bottom). The elemental Mg and Sb peaks are clearly observed in  $\text{Mg}_{3+x}\text{Sb}_2$  samples with  $x = 0.2$  and  $-0.1$ , respectively. This shows the range of nominal Mg content ( $-0.1 < x < 0.2$ ) explored in this study is sufficiently large to investigate both of the two distinct thermodynamic states: Mg-excess and Sb-excess.

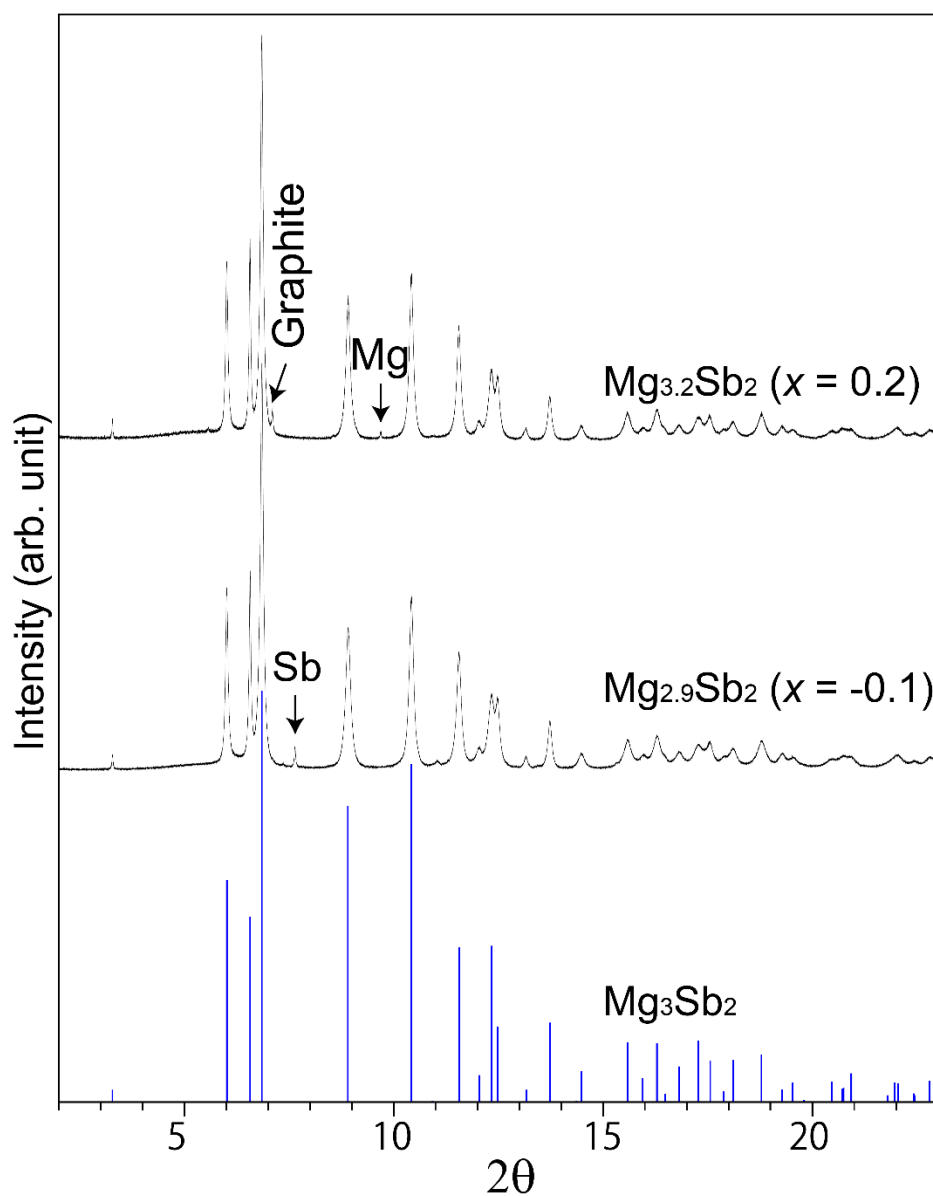


Figure S4. High-resolution synchrotron powder diffraction data of  $\text{Mg}_{3+x}\text{Sb}_2$  ( $x = 0.2$  and  $-0.1$ ) samples. The hot-pressed samples were grinded into powders after all the transport measurements and put into capillary for synchrotron. The measurements were conducted with the wavelength of  $0.414537 \text{ \AA}$ . Elemental Mg is observed in the sample of  $x = 0.2$  (Mg-excess) and elemental Sb is observed in the sample of  $x = -0.1$  (Sb-excess) as expected. Mg-excess sample contains small amount of Graphite, which is likely be a contamination during the sample preparation since no such peak is observed in Figure S3.

Table S1. Lattice constants obtained from the data shown in Figure S4 using the General Structure Analysis System (GSAS-II). Considering this and the elemental analysis shown in Table S2, there is a small phase width of  $\text{Mg}_3\text{Sb}_2$  but no indication of large Mg solubility. The significant peak broadening presumably due to the small grain size and large strain (most likely due to the grinding) makes the reliable Rietveld refinement unable and further structure analysis such as Mg occupancy could not be performed.

This difficulty of obtaining detailed structure analysis increases the importance of phase boundary mapping in nominal composition space to explore all the accessible thermodynamic states.

Nominal composition	a (Å)	c (Å)
$\text{Mg}_{3+x}\text{Sb}_2$ ( $x = 0.2$ )	4.5614(1)	7.2381(2)
$\text{Mg}_{3+x}\text{Sb}_2$ ( $x = -0.1$ )	4.5610(1)	7.2360(2)

Table S2. Elemental analysis by Energy dispersive spectroscopy (EDS) and wave dispersive spectroscopy (WDS) implies that the difference in the actual Mg content of Mg-excess and Sb-excess samples be drastically smaller than reported Mg solubility in ref [47], showing over 9 % of Mg solubility in  $\text{Mg}_3\text{Sb}_2$ . Due to the finite detection area, the small difference in Mg contents detected in EDS and WDS could simply arise from the elemental Mg which exists in the  $\text{Mg}_{3.2}\text{Sb}_2$  as shown in Figure S3 and S4.  $\pm$  shows the typical accuracy (2%) of the measurement.

	$\text{Mg}_{3.2}\text{Sb}_2$	$\text{Mg}_{2.9}\text{Sb}_2$
EDS	$\text{Mg}_{2.93\pm 0.06}\text{Sb}_{2.06\pm 0.04}$	$\text{Mg}_{2.92\pm 0.06}\text{Sb}_{2.08\pm 0.04}$
WDS	$\text{Mg}_{3.070\pm 0.06}\text{Sb}_{1.930\pm 0.04}$	$\text{Mg}_{3.049\pm 0.06}\text{Sb}_{1.951\pm 0.04}$